Construction and Building Materials 442 (2024) 137591

Contents lists available at ScienceDirect

Construction and Building Materials

journal homepage: www.elsevier.com/locate/conbuildmat

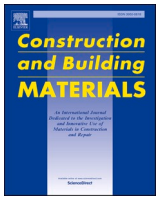

Enhancement of mortar's properties by combining recycled sand and limestone calcined clay cement

Ahmad Jan [a], Lucia Ferrari [a,*], Villiam Bortolotti [a], Nikola Mikanovic [b], Mohsen Ben-Haha [b], Elisa Franzoni [a]

[a] DICAM – Department of Civil, Chemical, Environmental and Materials Engineering, University of Bologna, Via Terracini 28, Bologna 40131, Italy
[b] Global R&D, Heidelberg Materials AG, Oberklamweg 2-4, Leimen 69181, Germany

ARTICLE INFO

Keywords:
Limestone Calcined Clay Cement (LC^3)
Recycled Fine Aggregate
Porosity
Capillary absorption
Low field Time Domain- Nuclear Magnetic Resonance (TD NMR)

ABSTRACT

The use of Recycled Fine Aggregate (RFA) combined with Limestone-Calcined Clay Cement (LC^3) is one of the low-carbon options for replacing ordinary mortar, leading to an eco-friendly and sustainable construction material, and providing a solution for waste management. In this paper, a comprehensive investigation concerning the mechanical properties and microstructural characteristics of LC^3 mortar, using different proportions of limestone, calcined clay, cement clinker, and two types of RFA (namely RS1 and RS2), was carried out. The results highlight that a binder with 17.55 wt% calcined clay, 8.77 wt% limestone, and 73.68 wt% CEM I shows superior mechanical properties compared to CEM I with both natural sand and high-quality recycled sand, and similarly it shows better mechanical properties than CEM II at all levels of substitution of natural sand with recycle sands of high and normal quality. The replacement of commercial cement with LC^3 mitigates the negative impact of RFA on water absorption, enhances pore size distribution, reduces total porosity, and boosts mechanical strength. The combination of RFA with LC^3 is an effective approach to reduce the environmental impacts of cement production, to well manage wastes generated by construction and demolition, and to improve material's performances.

1. Introduction

Sustainable development entails balancing economic, environmental, and social concerns while implementing a circular economy model aiming at prolonging materials' lifetime, reducing waste, preserving resources, and mitigating environmental degradation for the benefit of current and future generations. For this objective, on the one hand, solutions are needed to reduce the dramatic environmental impact of Ordinary Portland Cement (OPC), whose demand is rapidly increasing, and statistical trend estimation shows an expected increase from ~4.3 billion metric tons in 2015 to ~6.1 billion metric tons per year in 2050 [1]. The environmental problems associated with the OPC manufacturing process, including significant energy consumption and CO_2 emissions, are well recognized [2]. In addition, the production of OPC consumes a huge quantity of natural resources and contributes to greenhouse effect, as 1 ton of OPC releases about 1 ton of CO_2 and consumes about 1.7 tons of raw natural materials [3]. Due to the increasing world population and expansion of construction industries in developing countries, demand for OPC is estimated to increase globally by 4.5 % per year [4]. Therefore, the demand for the modification of the current concrete production process into an eco-friendly and sustainable one is increasing day by day.

To reduce cement clinker production, the use of Supplementary Cementitious Materials (SCMs) could be a valid alternative and viable approach [5]. Many waste materials rich in alumina and silica can contribute to the C-S-H and C-A-S-H formation, through the reaction with calcium hydroxide generated during the hydration of OPC, and can be employed as a partial replacement of OPC [6]. Furthermore, SCM can produce construction materials with enhanced mechanical and durability properties, with additional environmental improvements [5]. Despite of the various advantages associated with conventional SCMs, such as ground granulated blast furnace slag (GGBFS) and fly ash, on one side, the rising environmental concerns associated to coal utilization have limited the fly ash availability, and on the other side, the global production of GGBFS is less than 10 % of the total cement production [7].

* Corresponding author.
E-mail address: lucia.ferrari9@unibo.it (L. Ferrari).

https://doi.org/10.1016/j.conbuildmat.2024.137591
Received 3 June 2024; Received in revised form 12 July 2024; Accepted 23 July 2024
Available online 29 July 2024

To overcome the limited availability of SCMs, Limestone Calcined Clay Cements (LC^3) seems to be a promising alternative, as both limestone and clay are abundantly available across the globe [7,8]. The production process of LC^3 requires less amount of energy and reduces the CO_2 emission up to 40 % in comparison to OPC [9]. The calcination of kaolinitic clays generates metakaolin by the dehydroxylation of kaolin through a heat treatment process [10,11]. Due to the pozzolanic nature of metakaolin, when mixed with cement and water, it produces C-A-S-H, AFm and ettringite phases because of reaction with water, sulphate and portlandite [12,13]. Similarly, the limestone employment in OPC produces hemi- and mono-carboaluminate phases due to the reaction of calcite with C_3A present in clinker [14,15]. In LC^3 binder, metakaolin's aluminate interacts with calcite, promoting the development of carboaluminate phases [16]. The primary benefit of LC^3 is in its ability to be manufactured with clinker percentages that range from 50 % to 64 %, as proposed in the standard EN 197–5:2021, all without compromising mechanical performance [17]. However, workability of LC^3 fresh mixes was shown to be a technical issue that deserves further analysis to allow the application in construction [18–24]. Moreover, superplasticizer polymer structure and dosages still need to be optimised to achieve suitable rheological properties and workability retention [25–32].

The mechanical strength of LC^3 is a critical parameter that influences its performance in various applications. While main findings specify that the 28-day compressive strength of LC^3 is comparable to that of OPC made with similar clinker, the results at different ages fluctuate to some extent. Generally, the 3-day compressive strength of LC^3 is slightly lower than that of OPC but higher than that of slag or fly ash blended cements, while the 7 and 28 days LC^3 strength has been reported to match or exceed that of OPC [33,34]. Preliminary findings suggested that factors including particle size, clinker percentage, thermal activation process, and alkali content substantially affect the strength development process [35,36]. The analysis of the porous structure of LC^3 hardened at 28 days showed that finer pores are developed in comparison to OPC and these significantly improve durability [37–43].

On the other hand, solutions are needed for Construction and Demolition (C&D) waste [44], to reduce their landfill disposal, which is a significant issue for environment and society. Every year a huge quantity of waste from C&D activities is produced in Europe. This quantity was about 798 million tons in 2020 and continues to increase [45]. Simultaneously, the growth in population and urbanization has contributed to an increase in the demand for river sand, especially in the Asian region [46]. The global demand and consumption of river sand is approximately 32–50 billion tons per annum [47] and causes significant damage to the coastal areas and their ecology [48]. Considering that the sand from deserts is finer and is not suitable to be employed as a construction material, and the manufactured sand or crushed sand from the hard rock quarries will cause the natural resources depletion, the best alternative seems the use of recycled sand (RS) manufactured from C&D waste for the production of new construction materials. This has the potential for playing an important role in reducing the natural sand demand and pollution caused by C&D waste. Several research studies have been conducted on the assessment and compatibility of recycled aggregates with OPC to evaluate their impact on the mechanical performance of mortars and concrete and usually these findings indicate a detrimental effect on the workability [49], mechanical strength [50,51], long-term properties [52,53] and the overall performance of final construction materials [54–56]. Thus, the large-scale practical application of recycled aggregates is still challenging due to the above-mentioned negative effects that still need to be solved. In addition, several methods have been employed by scholars for the enhancement of the overall performance of mortars and concrete with recycled aggregate, with a primary emphasis on the treatment of recycled aggregate, e.g., by the removal of the cement mortar attached to recycled aggregate [57,58], acid pickling treatment, improvement by CO_2-curing and polymer coating, which are all generally employed techniques for enhancing recycled aggregate performance [59,60]. Moreover, the mechanical properties of recycled aggregate can be improved up to a certain level by the use of nanomaterials and mineral admixtures [61,62]. However, the above methods employed for the improvement of recycled aggregates performance are generally time consuming and costly [63]. From the above discussion it can be concluded that considerable research study has been carried out regarding the use of recycled aggregates in ordinary mortar and concrete. However, while large aggregates (gravel) can be reused easily, fine aggregates (sand) present challenges. The hydrate layer around the sand particle absorbs water, with the water absorption coefficient varying by fraction size [64], and mortar workability is strongly affected by the recycled sand's moisture condition [65]. The mechanical strength is reduced up to 60 % when RFA substitute standard sand [66] and it was shown that the use of 100 % RFA in concrete significantly diminishes the durability [67]. Therefore, incorporating RS into LC^3 blend seems to be a promising combination in terms of sustainability and performances, despite limited research studies [9,68–70].

For these reasons, in the present work, the combination of recycled construction material from waste concrete with a low-carbon binder was analysed as an efficient method of sustainable and greener construction industry development. To establish the practical viability of mortar containing recycled sand (RS) and LC^3, the assessment of material properties in both the fresh and hardened states if very important. This research study was carried out to evaluate the effect of LC^3 on the rheological and mechanical properties as well as the water absorption capability of different mortar mixes. Specifically, the substitution effect of OPC with LC^3, prepared with different proportions of clinker, calcined clay and limestone, and the replacement of Natural Sand (NS) by two types of recycled sand (RS1 and RS2) at 50 vol% and 100 vol% rate was evaluated. The initial focus was kept on the workability and mechanical strength, then the study was extended to evaluate the durability properties through capillary water absorption and 24 hours total water absorption. Porosity assessment by Mercury Intrusion Porosimeter (MIP) at 28 days was also performed. In addition to the classical methodologies to evaluate pore size distribution of hydrated cement, low field Time Domain- Nuclear Magnetic Resonance (TD NMR) at 28 days was also performed, as in last decades this technique affirmed its potential as a non-destructive and non-invasive technique to analyse construction materials. Several studies detailed the possibility of evaluating cement hydration by a low field approach to detect the water confined in pores of different sizes [71–73]. The main finding of this study is the significant improvement of mechanical strength and durability performances by combining LC^3 with recycled sand.

2. Materials and methods

2.1. Materials and their characterization

Two commercial Portland cements, CEM I 52.5 R and CEM II/A-LL 52.5 N containing 12 % of limestone, both having density equal to 3080 kg/m^3, were used as reference binders. Their oxide compositions were detected by X-ray fluorescence (XRF) analysis (Table 1). Calcined clay (CC) and limestone (LS), having densities 2890 and 2720 kg/m^3, respectively, were employed in different ratios to formulate the following LC^3 cements: LC3—50 2:1, LC3—50 1:1, LC3—70 2:1, whose compositions are reported in Table 2. Particle Size Distribution (PSD) of CEM I and CEM II was determined by laser diffraction with a Malvern Mastersizer 3000, in isopropanol, while limestone and calcined clay were tested in water by a Malvern Hydro 2000MU (A), in water (Fig. 1). The analysis showed comparable particle size distribution for the powders except for LS, which exhibits coarser particles.

For the mortars' preparation, natural sand (NS) and two types of recycled sand (RS1 and R2) were employed. Natural sand is manufactured crushed sand from natural quartz rocks. The two recycled sands were produced from demolished concrete in industrial trials using advanced concrete recycling techniques. Similarly to conventional

Table 1
XRF Oxide composition analysis of CEM I, CEM II and CC (LOI: loss on ignition).

Material	Chemical compound (%)									LOI 1050 °C (%)	Sum (%)
	Al_2O_3	CaO	Fe_2O_3	K_2O	MgO	Na_2O	SiO_2	SO_3	Other oxides		
CEM I	5.1	62.7	3.2	1.0	1.9	0.07	19.2	3.3	0.5	2.5	99.5
CEM II	4.8	61.4	3.0	1.0	1.7	0.06	18.1	3.2	0.5	5.5	99.6
CC	25.8	1.0	8.9	0.2	0.2	0.0	60.2	0.1	1.3	2.4	100

Table 2
Binder mix proportion (wt%).

Binders	CEM I (%)	CEM II (%)	LS (%)	CC (%)
CEM I	100	0	0	0
CEM II	0	100	0	0
LC3–50 2:1	52.63	0	15.79	31.58
LC3–50 1:1	52.63	0	23.68	23.69
LC3–70 2:1	73.68	0	8.77	17.55

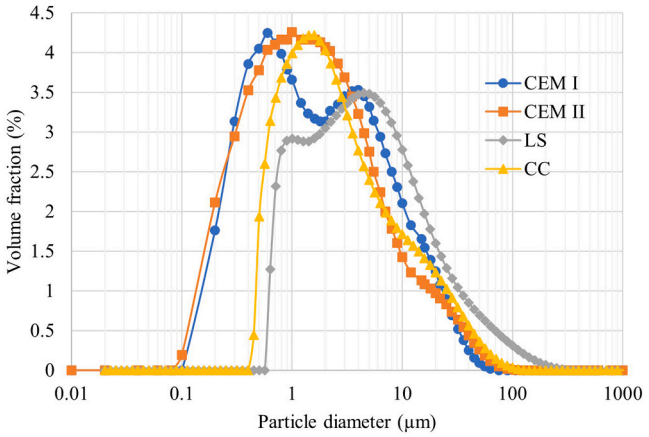

Fig. 1. Particle size distribution of binding materials.

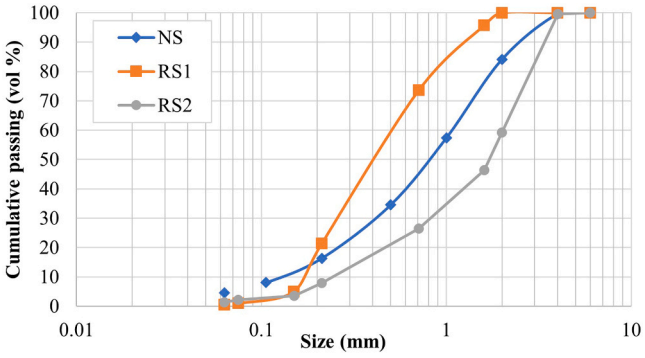

Fig. 2. Particle size distribution of NS, RS1 and RS2.

Table 3
Physical-chemical properties of NS, RS1 and RS2.

Sand	Oven-dried particle density (g/cm^3)	Water absorption (%)	Blue methylene value MB (g of dye solution/kg of sand)	Chloride content (Cl^-, wt %)	Sulfate content (SO_4^{2-}, wt%)	TOC (mg C/kg sand)
NS	2.66	0.4	0.24	0.019	0.007	7.84
RS1	2.27	4.7	0.40	0.029	0.188	26.85
RS2	2.16	6.9	0.35	0.026	0.152	29.18

recycling process, advanced recycling trials begin with the removal of any non-concrete materials, followed by primary crushing to reduce the demolished concrete into smaller pieces. The subsequent step, often referred as selective separation, employs mechanical forces to separate the cement paste from the aggregates. As selective separation technologies are still in development, further details cannot be provided. After the selective separation stage, specialized equipment is used for screening and separating the different particle sizes, resulting in relatively clean fine and coarse aggregates, and recycled cement paste [74]. The particle size distribution of NS, RS1 and RS2 was detected by sieve analysis according to EN 933–1 standard [75], relative density and water absorption according to EN 1097–6 [76] standard, and methylene blue tests according to EN 933–9 standard [77], while chloride and sulphate contents were obtained by ion chromatography (Dionex ICS 1000, ThermoFisher, US). Total Organic Carbon (TOC) results were obtained through an analyzer TOC 5000 A, Shimadzu, Japan. The results are reported in Fig. 2 and Table 3. Fig. 3 reports photos of the materials.

In addition to these techniques, an original test to detect the occurrence of delayed water absorption of the 3 sands was performed. This consists in placing the dry sand in graduated cylinders (accuracy of 1 ml) reaching a volume of nearly 40 ml, adding water up to nearly 80 ml and leaving it for 24 hours to detect the water absorption over time. No change in water level was observed after 24 hours, suggesting that water absorption by sand was instantaneous. Based on these results, no pre-wetting of sand was carried out in mortar preparation, as no delayed water absorption and no significant difference were expected. Moreover, the TD NMR was applied to evaluate the open porosity and the pore size distribution of the different types of sand. The dry material was kept immersed in water for 24 hours, then extracted, filtered and analysed by logarithmic CPMG sequence, that is described in the methods' section 2.4.2 of this paper. Results are Fig. 4.

Material characterisation shows high water absorption for RS, while it is almost negligible for NS, consistently with the higher particle density of NS. Methylene blue test values, TOC, chloride and sulphate content are higher for the recycled sand than for the natural sand, but still below the threshold reported in the standard EN 12620 for aggregate's quality. PSD of NS is intermediate between RS1 and RS2. TD NMR characterisation confirms the presence of residual cement paste (C-S-H gel) in RS, as water-filled-pores with relaxation time of 0.2–0.3 ms were detected, that are assigned to gel pores of few nm. A peak corresponding to similar relaxation time is not visible in NS, revealing that RS1 and RS2 contain additional fine pores that are responsible of supplementary water absorption. Overall, RS1 appears to contain less residual cement paste and hence to be of better quality than RS2 sand.

2.2. *Mortars' formulations*

The mortars were prepared using the different binders shown in Table 2 and substituting NS with RS1 and RS2 in the proportions 50 vol % and 100 vol%, according to the formulations reported in Table 4. It is noteworthy that the substitution of natural sand with the recycled ones was carried out by volume rather than by mass, to take into account the different particle density of the recycled sands. This was considered very important to ensure that the volume fraction of cement paste in all the mortars remained the same and sand substitution did not significantly

Fig. 3. Pictures of NS (left), RS1 (middle) and RS2 (right).

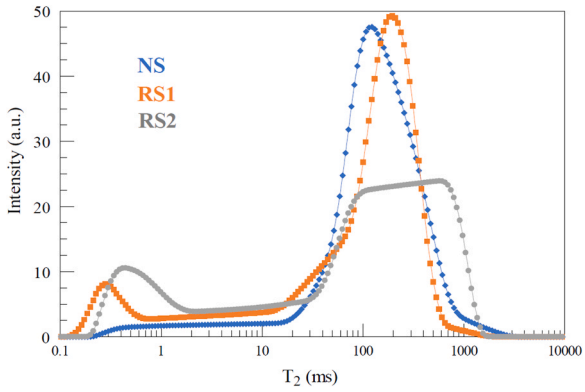

Fig. 4. T_2 relaxation time distribution of water-saturated sands obtained by logarithmic CPMG TD NMR sequence.

affected workability. In some preliminary tests that are not reported here for brevity's sake, also the formulation of the binders was performed by volume replacement method, but no significant differences were observed between binders formulated by mass or by volume in terms of workability and mechanical strength of mortars. Moreover, considering that calcined clay contains some internal porosity, the procedure of volume substitution of clinker by calcined cay may be affected by errors, due to the lack of an established method to measure geometrical density of powders in saturated surface dry conditions. The mortars were prepared using the three sands (NS, RS1 and RS2) at different substitution levels of RS (50 vol% and 100 vol%) with five different binders (CEM I, CEM II, LC3—50 2:1, LC3—50 1:1 and LC3—70 2:1), and their fresh and hardened state properties were evaluated by different techniques. These substitution rates of NS with RS1 or RS2 were selected to establish clear and distinct trends in sand substitution, as this approach allowed a more effective evaluation of the impact of the 5 different binders. A polycarboxylate ether-based superplasticizer (SP),

Table 4
Formulation of the mortars prepared in this study.

	Binder				Total water		Sand			
Labels	CEM I (g)	CEM II (g)	LS (g)	CC (g)	W_{eff} (g)	W_{sand} (g)	NS (g)	RS1 (g)	RS2 (g)	SP (g)
CEM I-NS	450	-	-	-	225	0	1350	-	-	2.7
CEM II-NS	-	450	-	-	225	0	1350	-	-	2.7
LC3–50 2:1-NS	237	-	71	142	225	0	1350	-	-	5.8
LC3–50 1:1-NS	237	-	107	107	225	0	1350	-	-	4.9
LC3–70 2:1-NS	332	-	39	79	225	0	1350	-	-	4.5
CEM I–50RS1	450	-	-	-	225	27	675	584	-	2.2
CEM II–50RS1	-	450	-	-	225	27	675	584	-	2.2
LC3–50 2:1–50RS1	237	-	71	142	225	27	675	584	-	5.4
LC3–50 1:1–50RS1	237	-	107	107	225	27	675	584	-	4.5
LC3–70 2:1–50RS1	332	-	39	79	225	27	675	584	-	4.1
CEM I–100RS1	450	-	-	-	225	54	-	1168	-	1.8
CEM II–100RS1	-	450	-	-	225	54	-	1168	-	1.8
LC3–50 2:1–100RS1	237	-	71	142	225	54	-	1168	-	4.9
LC3–50 1:1–100RS1	237	-	107	107	225	54	-	1168	-	4.1
LC3–70 2:1–100RS1	332	-	39	79	225	54	-	1168	-	3.6
CEM I–50RS2	450	-	-	-	225	38	675	-	554	1.8
CEM II–50RS2	-	450	-	-	225	38	675	-	554	1.8
LC3–50 2:1–50RS2	237	-	71	142	225	38	675	-	554	4.0
LC3–50 1:1–50RS2	237	-	107	107	225	38	675	-	554	3.0
LC3–70 2:1–50RS2	333	-	39	79	225	38	675	-	554	2.7
CEM I–100RS2	450	-	-	-	225	76	-	-	1109	0.6
CEM II–100RS2	-	450	-	-	225	76	-	-	1109	0.6
LC3–50 2:1–100RS2	237	-	71	142	225	76	-	-	1109	2.6
LC3–50 1:1–100RS2	237	-	107	107	225	76	-	-	1109	2.0
LC3–70 2:1–100RS2	332	-	39	79	225	76	-	-	1109	1.6

with a solid content of 22 %, provided by CHRYSO-SAINT GOBAIN laboratories, was used to adjust the fluidity of mortars. The water-to-cement (w/c) ratio was consistently maintained equal to 0.5 for all the mix proportions throughout the research study and the SP dosage was adjusted to reach target workability. Of course, the recycled sands exhibit a non-negligible water absorption hence they are expected to cause a significant water depletion from the fresh mixes. This was compensated by adding to the mixes the amount of water necessary to bring all the aggregates to the saturated surface dry condition, as currently done in concrete manufacturing. Table 4 reports the mass of aggregates in dry condition, the mass of water necessary to bring them to saturated surface dry condition (W_{sand}) and the mass of effective water (W_{eff}), the latter corresponding to a water to cement ration equal to 0.5. The curing of the samples was carried out in a humid chamber at relative humidity >95 %. The mix proportions of the mortars and their labels are presented in Table 4.

2.3. Mortars' preparation and curing

The mixing (in a Hobart mixer) and casting of the mortars were conducted at laboratory temperature, and prismatic samples ($4\times4\times16$ cm^3) were prepared and cured according to EN 1015–11 [78].

2.4. Methods

2.4.1. Fresh state properties

Workability of mortar was detected immediately after mixing by flow table test according to standard ASTM C1437–20 and an average mortar spread of (21±1) cm after 25 table drops was settled as target. SP dosage was consequently adjusted.

2.5. Hardened state properties

The mechanical strength of mortars was evaluated according to EN 196–1 standard [79] at 2 and 28 days. The selected the curing ages conform to the requirements of the standard EN 197–1 [80], that describes cement classes according to the compressive strength at 2 and 28 days. The capillary water absorption test at 28-days curing was carried out on mortars according to EN 1015–18 [81]. The specimens were dried in ventilated oven at 110°C for 24 hours and then placed in desiccation chamber for 24 hours to remove all their moisture. The mass after 10 minutes (W10) and after 90 minutes (W90) in contact with water were recorded. The capillary coefficient (C), measured in $kg/(m^2{\cdot}min^{0.5})$, was calculated according to the following equation:

$$C = 0.1 \bullet (W90 - W10)$$

Then, 24 hours water absorption test was carried out on the same samples, according to ASTM C 642 [82] standard. Mercury intrusion porosimeter (MIP) technique was employed for the characterization of pore structure and porosity of hardened mortars. After 28 days of curing, the specimens were oven dried at 110 °C for 24 hours and a fragment having mass between 0.8 and 0.9 g was analysed with a Thermo Scientific Pascal series mercury porosimeter (140 and 240) instrument.

Porosity was also evaluated by TD NMR experiments performed on mortar fragments extracted after the mechanical compressive strength test at 28 days. The NMR equipment is composed of a permanent magnet (ARTOSCAN, Genova, Italy) providing a constant a magnetic field $B_0 \approx 0.2$ T (corresponding to ^{1}H Larmor frequency ≈ 8 MHz) and an NMR console (Stelar s.r.l., Mede, Italy). A 20 mm probe was used to enable the measurement of fragments of nearly 1–1.5 cm in diameter. The detection of the T_2 relaxation time was performed by Carr–Purcell–Meiboom–Gill (CPMG) sequence with 256–512 no. of echoes, depending on the saturation level of the samples, with an echo time of 60 μs and 500 scans. The T_2 quasi-continuous distributions were computed by the software UpenWin [83], developed by the NMR group at the University of Bologna.

3. Results and discussion

3.1. Fresh state properties

The SP amounts required for different mixtures to obtain the desired workability (21±1 cm after 25 falls) are shown graphically in Fig. 5. It has to be mentioned that preliminary tests were carried out by substituting NS with the same mass of RS1 or RS2. By this approach, the amount of SP required to obtain target workability of mortars was extremely high, reaching values exceeding 5 %. Contrarily, it can be observed that for all substitution levels of NS with RS1 and RS2 by volume, the required SP dosage slightly decreases with increasing sand substitution quantity. These findings indicate that when substituting natural sand with recycled ones, the rheological properties of the mortar can remain basically unaffected if the mix design calculation is carried out by volume instead of by mass. This is because, in rheology, the volume occupied by the grains plays a more crucial role than the mass in determining the flow properties of a mix. One hypothesis about the lower SP demand for increasing amounts of recycled sand can be the additional water for the compensation of high-water absorption (4 % and 7 %) of RS1 and RS2 and that counterbalance the calcined clay higher SP need. However, the water absorption test was carried out to study the recycled sand water absorption behaviour with respect to time and the result indicate that there is no change in the water level and absorption with respect to time. One hypothesis could be that the test used to verify the saturated surface area of aggregates slightly overestimates the amount of water needed for workability. However, this goes beyond the scope of this study. It can be observed that CEM I and CEM II required less SP compared to LC^3 binders across all the substitution levels of sand and the demand reaches 1.30 % for LC3–50 2:1 binder, which contains the highest amount of CC among all the binders, hence the CC has a negative effect on the workability and the SP demand for a targeted workability increases with the amount of CC. Several authors have reported the same tendency hence these findings are in agreement with previous literature [84], and a recent study proposed that the impact of CC on SP dosage is due to the high specific surface area of calcined clay [85].

3.2. Mechanical strength

The compressive and flexural strength of mortars with different binders and different RS1 and RS2 replacement levels (50 % and 100 %) with respect to curing age (2 and 28 days) are shown in Fig. 6 and Annex A.

Focusing on the mortars with NS, the performance of LC^3 in comparison with the reference cements can be observed. From Fig. 6(a) and (c) it can be seen that at 2 days all LC^3s exhibit mechanical strength much lower than CEM I, and LC3–50 is even worse than CEM II, which is

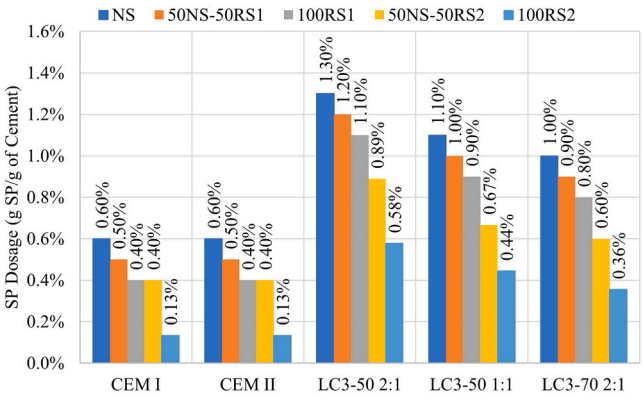

Fig. 5. SP dosage required to reach targeted workability of mortars with different binder.

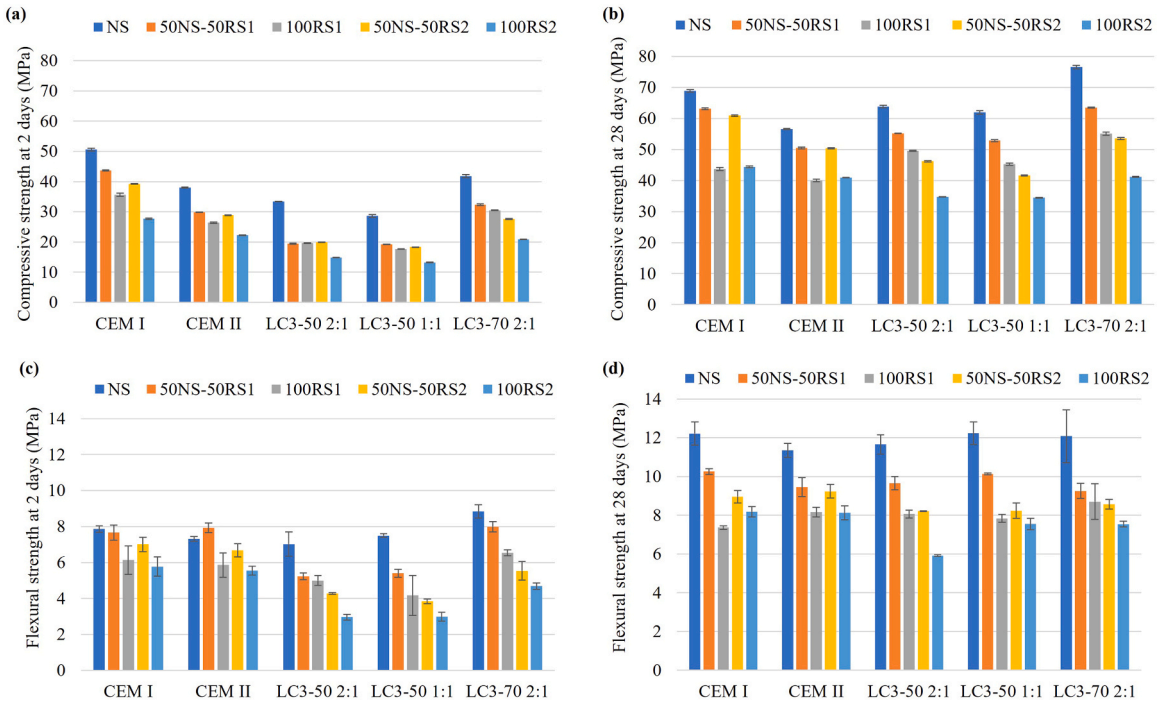

Fig. 6. Mechanical strength obtained with different binders at various RS1 and RS2 substitution rates. (a) Compressive strength at 2 days, (b) Compressive strength at 28 days, (c) Flexural strength at 2 days, (d) Flexural strength at 28 days.

considerably less performing than CEM I. However, the 28 days strength of all LC^3s is better than CEM II and in the case of LC3–70 2:1 even better than CEM I. This is because of the effect at the early-stage hydration process of LS and CC, which slows down the strength development of the LC^3 mortars compared to OPC [42,86,87]. As the hydration of the binders progresses, the effect of pozzolanic reaction of CC with portlandite enhances the strength development [88–90]. Besides this, in previous literature it was reported that the pore structure becomes more refined with the aging of the samples for higher kaolinite contents binders, which ultimately contributes to higher strength development at later age compared to OPC binders [89].

Focusing on the effect of recycled sands, it can be observed that for all the binders, an identical trend of reduction of compressive and flexural strength with the replacement of NS with recycled sands was found, as expected. However, when comparing the 28 days compressive strength for NS and RS1, the LC3-70 2:1 binder exhibits superior mechanical strength compared to both CEM I and CEM II. In fact, LC3–70 2:1 has the highest 28 days compressive strength compared to all the investigated binders and improves the 28 days compressive strength of LC3–70 2:1-NS by 11 % compared to CEM I-NS and 35 % compared to CEM II-NS. Similarly, the LC3–70 2:1–50RS1 compressive strength improved by 0.5 % compared to CEM I-50RS1 and 25 % compared CEM II-50RS1 and in the case of LC^3-70 2:1–100RS1 the improvement reached 25 % compared to CEM I-100 % RS1 and 37 % compared to CEM II-100RS1. Moreover Fig. 6(b) provides a visual representation that clearly shows the superior compressive strength of the LC3–70 2:1 binder in comparison to CEM II across all levels of RS1 and RS2 replacement. Fig. 6(d) represents the 28 days flexural strength and there is no discernible trend of enhancement in flexural strength relative to CEM I across various levels of sand substitution. However, the results are comparable with CEM I and CEM II. Also, the conducted investigation reveals that mechanical strength is impacted by sand substitution. Specifically, at 28 days, commercial cements are more affected by the substitution percentage, while LC^3s are more affected by sand quality.

3.3. Water absorption

The capillary water absorption behavior as a function of time can be ascribed to open porosity and pore connectivity [91] and is described by the capillary coefficient C of the mortars, reported in Fig. 7. The capillary coefficient seems mainly affected by two parameters: the CC content in the binder and the substitution rate/quality of the recycled sands. Focusing on the role of the binder (capillary coefficients of mortars with NS in Fig. 7), a positive reduction in the capillary coefficient was observed for binders containing calcined clay and limestone. From Fig. 7, it can be also seen that the capillary coefficient increases by increasing the substitution level of sand and depending on the type, passing from NS to RS1 and RS2. These results indicate that capillary coefficient is directly dependent on the quantity and quality of sand. However, notably, the CC content present in the binder not only has a positive impact on the capillary coefficient, but even compensates for the negative effect of water capillary absorption caused by the use of RS1 and RS2. For instance, the capillary coefficient of LC3–70 2:1-NS is reduced by 21 % compared to CEM I-NS and 33 % compared to CEM II-NS. Similarly, the capillary coefficient of LC3–70 2:1–50RS1 is

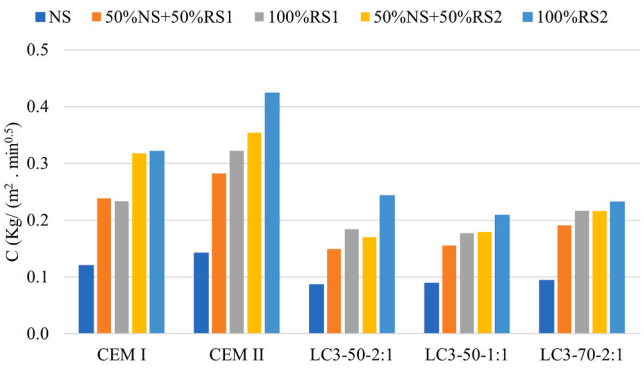

Fig. 7. Capillary coefficient (C) of the mortars with different binders and at different RS1 and RS2 percentage substitution.

reduced by 20 % compared to CEM I-50RS1 and 32 % compared to CEM II-50RS, in case of LC^3-70 2:1–100RS1 the capillary coefficient reduced by 8 % compared to CEM I-100 RS1 and 32 % compared to CEM II-100RS1. Furthermore, with use of RS2 LC3–70 2:1–50RS2 the capillary coefficient is reduced by 32 % compared to CEM I-50RS2 and 39 % compared to CEM II-50RS2, and in case of 100 % RS2 the capillary coefficient of LC3–70 2:1–100RS2 is reduced by 28 % compared to CEM I-100RS2 and 45 % compared to CEM II-100RS2 respectively. These findings highlight the critical role of binder's composition in determining the capillary coefficient. For example, the capillary coefficient of mortar containing LC3–50 1:1 and 100 % recycled sand of low quality (RS2) is lower than that of a mortar containing CEM I and only a 50 % substitution of NS with high quality recycled sand (RS1). This relationship has the potential to mitigate the negative effects associated with variations in sand type and substitution, providing improved performances in comparison with the commercial cements. It should be noted that LC^3s with recycled sands of any nature outperforms CEM II, which is probably one of the most diffused binders used in constructions.

The total water absorption measured after 24 hours of immersion of the specimens in deionized water is reported in Table 5. From Table 5, it can be observed that the water absorption percentage increases gradually with the increase of RS1 and RS2 replacement, and to a higher extent for RS2, which is more porous than RS1. This increment is expected, due to the higher water absorption of RS1 and RS2 compared to NS, being well known in the literature that recycled sand has higher proportion of old mortar with porous structure [63,92]. Both properties, i.e., mechanical strength and capillary absorption, are influenced by the porosity of the mortar fraction in the recycled aggregates.

Moreover, LC3–70 2:1 mortar has lower water absorption than CEM II for NS and RS1 and higher than CEM I for NS, RS1 and RS2. This is related to the refinement of pore structure due to pozzolanic reactions and development of secondary hydration products, [91] as well as fine particle size distribution of CC. Similarly, LC3–70 2:1–50RS2 has comparable water absorption with respect to CEM II-50RS2 and higher than CEM II-100RS2. These results indicate that the quality and quantity of recycled sand emerge as primary factors affecting water absorption, particularly at 24-hour.

The comparison between the capillary coefficients and 24-hour water absorption values of the mortars allows to make some important observations. While the total water absorption is dominantly controlled by the porosity present in the recycled sands, the speed of capillary absorption of water is mainly controlled by the nature of the binder, and in particular it is strongly reduced by LC^3, with an expected beneficial effect for durability.

3.4. Porosity evaluation

Upon comparison of water absorption results (Table 5) and total porosity results (Table 6), it can be observed that there is a directed correlation between total water absorption and porosity measured by MIP. The results from MIP are presented in Table 6 and Fig. 8(a, b, c, d, e). It can be observed that the substitution of the clinker with limestone and calcined clay changed the total volume of pores and specific pore volume.

Table 5
24-h water absorption calculation of mortars with different binders at RS1 and RS2 substitution levels 0 %, 50 %, and 100 %.

Sample ID	Water Absorption (wt%)				
	NS	50NS-50RS1	100RS1	50NS-50RS2	100RS2
CEM I	6.9	8.3	10.6	8.7	12.3
CEM II	7.9	9.7	11.6	9.5	12.6
LC3–50–2:1	7.3	9.5	11.7	9.8	13.5
LC3–50–1:1	7.9	9.7	12.1	11.1	13.8
LC3–70–2:1	7.3	8.7	10.8	9.4	13.3

Table 6
Total Porosity of different binders at different substitution level of RS1 and RS2 measured by MIP.

Binders	NS	50NS-50RS1	100RS1	50NS-50RS2	100RS2
	Porosity %				
CEM I	12.19	15.63	17.45	14.85	21.32
CEM II	14.41	15.35	18.89	16.58	23.53
LC3–50–2:1	14.06	16.86	17.97	16.89	17.82
LC3–50–1:1	14.03	14.84	17.89	17.46	18.66
LC3–70–2:1	11.61	15.50	17.44	15.64	18.74

Concerning the binder effect, the LC3–70 2:1 binder reduces the total porosity and refines the pore size distribution in comparison to CEM I and CEM II at all levels of NS substitution with recycled ones, except for LC3–70 2:1–50RS2 which is comparable to CEM I-50RS2. Hence, the mix containing 70 % of clinker and CC:LS=2:1 provides a dense structure and increases the overall performance of the LC3–70 2:1 binder in comparison to all the examined binders.

Concerning the sand substitution, recycled sand has a negative effect on the porosity, increasing it. From Table 6 and Fig. 8 it can also be observed that total porosity greatly depends on the quantity and quality of recycled sand, while pore size distribution seems to be mainly affected by the type of binder. RS2 produced a highly porous mortar compared to RS1 and NS, thus the overall performance of mortars with RS2 is worse than the others. For the mortar containing 50 % RS, the small size of the sample (0.8–1 g) may lead to local inhomogeneities, and the obtained data provide a less clear trend.

In summary, the MIP results indicate that LC3–70 2:1 exhibits the finest pores, while CEM II displays the largest ones. This observation potentially explains the differences detected in the measured total water absorption, capillary absorption coefficient and compressive strength.

The TD NMR results obtained on hardened mortars prepared with 5 different binders and 5 different sand compositions after 28 days of hydration are displayed in Fig. 9.

In all the analysed samples, the T_2 intensity distribution shows, as expected at 28 days according to [93], one main single peak around 0.2 ms, corresponding to the C-S-H water in pores having size of few nm. This pore size is below the limit of detection of MIP thus being not visible in previous plots of Fig. 8. Furthermore, the results obtained from MIP reveal a notable presence of pores ranging between 200 and 300 nm, suggesting a relaxation time T_2 within the range of 1–10 ms according to the literature [93]. Nevertheless, the TD NMR signal detected for pores of this size exhibits reduced intensity compared to the peak observed at 0.2 ms, indicating lower contribution to the variation of magnetisation from pores of 200–300 nm. These findings are consistent with the literature, which suggests that cement hydration leads to the consumption of capillary and interhydrate water, thereby refining the porous structure of the matrix [94].

Concerning the different binders, LC3–70 2:1 shows the finest water-filled pores, corresponding to the shortest T_2, while CEM II provides the largest pores, corresponding to the longest T_2, independently from the sand type and composition. This corresponds to the development of a finer porous structure of the cement gel in LC3–70 2:1 in comparison to CEM II and can directly explain the behaviour of these binders concerning the mechanical strength, where LC3–70 2:1 reached the highest compressive strengths and CEM II the lowest, independently from the sand type.

With the proposed NMR approach, only peak position, thus relaxation time distribution, can be discussed. As the signal amplitude is influenced by sample mass, and this was varying from one specimen to the other, thus remaining between 18 and 26 g, the peak's height is not

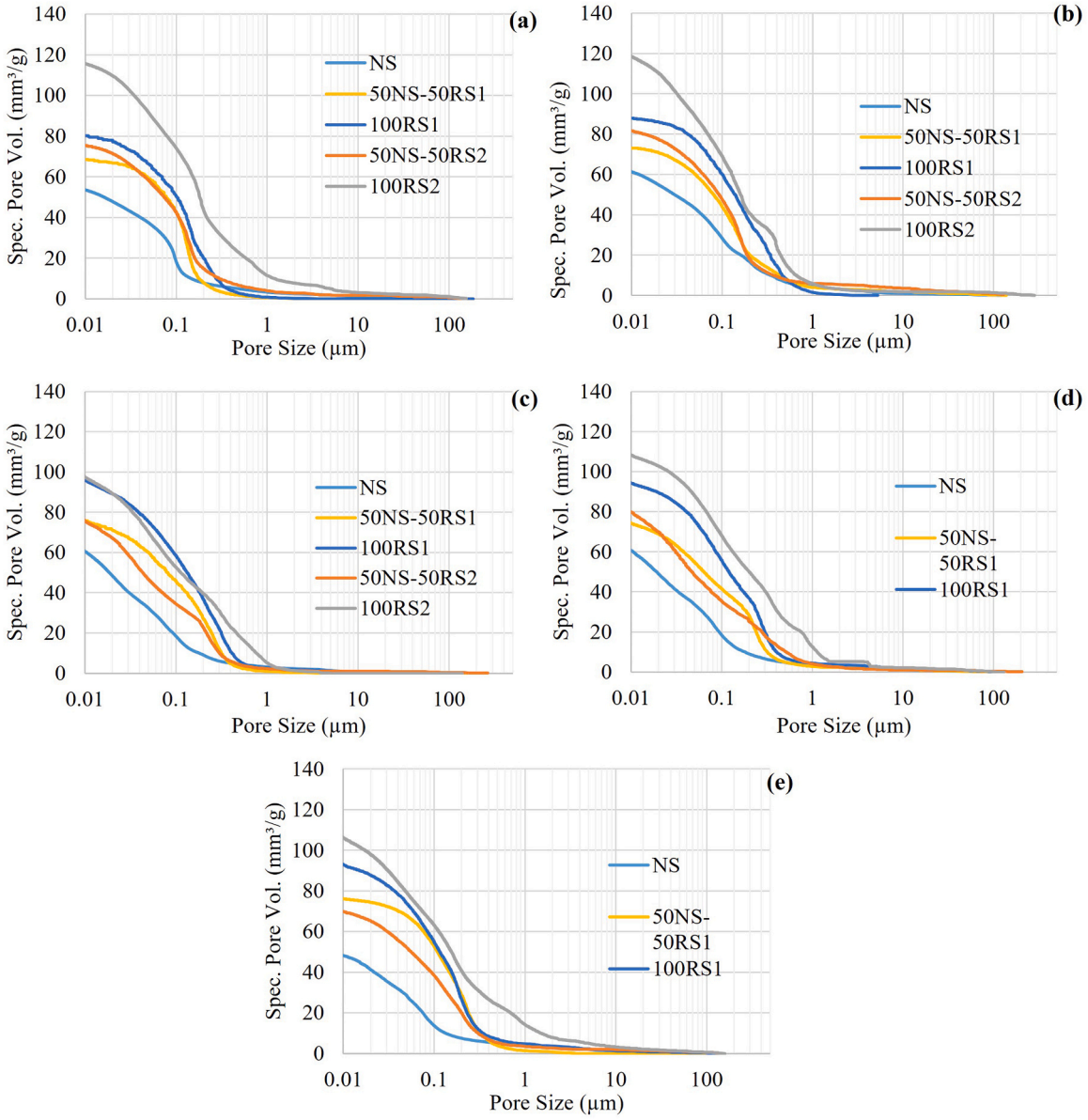

Fig. 8. Pore size distribution with respect to different substitution rate of RS1 and RS2 of different binders: (a) CEM I, (b) CEM II, (c) LC3–50 2:1, (d) LC3–50 1:1, (e) LC3–70 2:1.

discussed in this paper. The sand type and substitution rate seem to mainly contribute to the peak placed in the same range of C-S-H gel. However, the recycled sand, containing previously hardened paste from construction and demolition, mainly contributes to increase the amount of C-S-H pores whose signal is then overlapping with the freshly generated calcium silicate hydrate. In this condition, the binder type becomes the key parameter differentiating fine pores detection.

The porosity evaluation of mortars performed by MIP and TD NMR provides different range of pore sizes, as pores detected by TD NMR can be around few nm and this is below the detection limit of MIP instrument (7 nm). However, the two techniques confirmed the same classification of binders in regarding their pore size distribution and some calculations are proposed here to evaluate and compare the materials microstructure detected by the two techniques.

As the binder provides the main influence on fine pore size distribution, the following approach was applied to mortar containing natural sand only. The bulk density ρ_{bulk} was calculated as the ratio between the dry mass m_{dry} and the geometric volume V_{geom} of specimens used for water absorption:

$$\rho_{bulk} = \frac{m_{dry}}{V_{geom}}$$

The open porosity percentage measured by MIP, OP_{MIP}%, is the value reported in Table 6 directly obtained by the measurements, while the water absorption percentage, WA%, is the values reported in Table 5 measured after 24 hours of immersion of the specimens and calculated as the mass percentage increase due to water absorption. The mass of the sample analysed in NMR, m_{NMR}, is used to estimate the amount of water detected in mortar. First the water fraction available for hydration was calculated according to:

$$water\ fraction\ in\ mortar = m_{water}/(m_{water} + m_{sand} + m_{cement})$$

and this is equal to 0.11 for all standard mortar and mortars prepared with NS. Secondly, it was assumed that all the water introduced during mixing reacted to form hydrates, like C-S-H and others, and was detected with the performed TD NMR measurements. In this way, the amount of water in hydrates, $water_{hydrates}$, was roughly overestimated but it allows to generally calculate the amount of water in hydrates for each sample

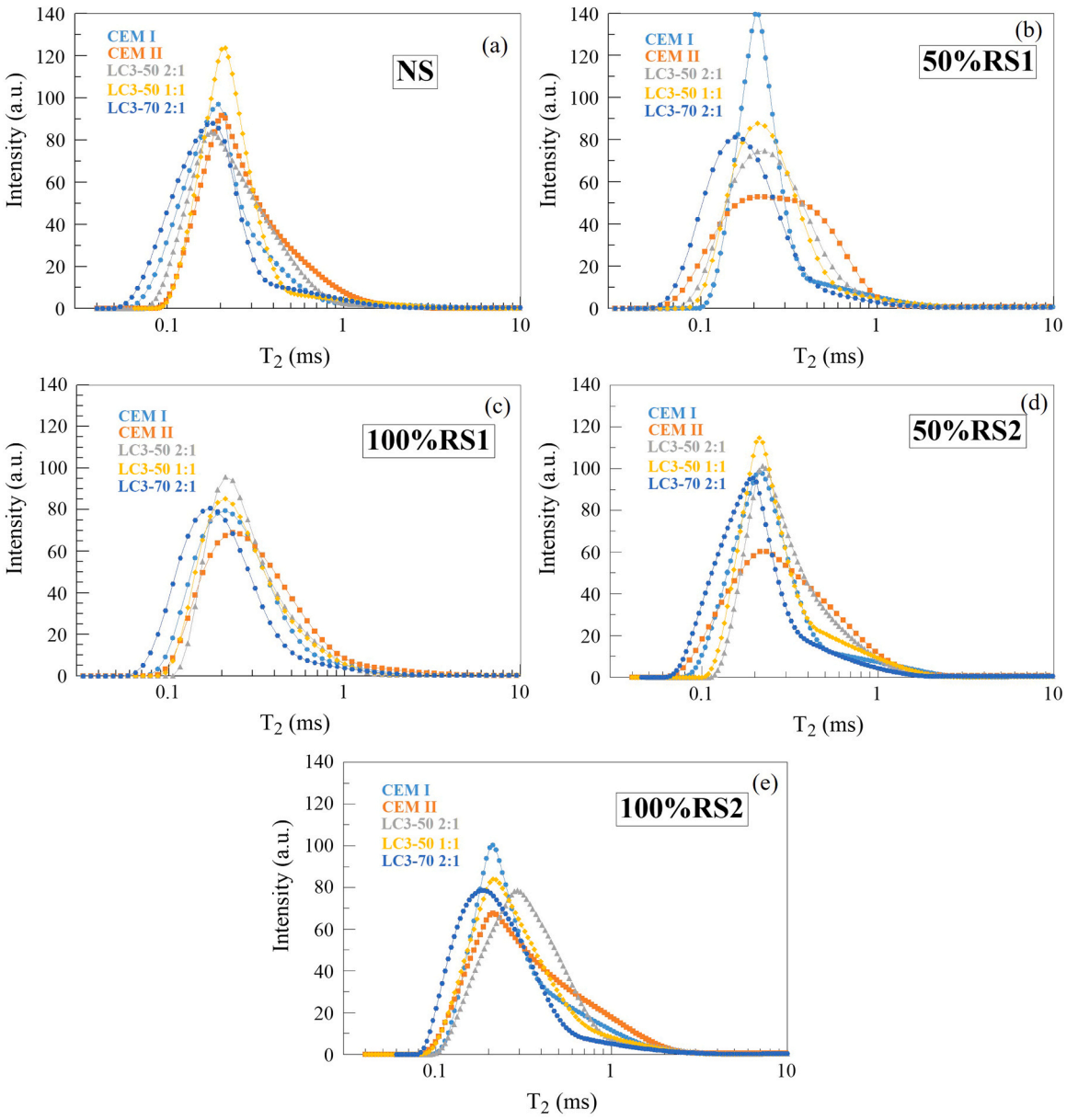

Fig. 9. The distribution of T_2 relaxation time measured at the curing state of mortars, prepared with 5 different binders mixed with 5 different sand composition, and hardened for 28 days. From the top: (a) NS, (b) 50 %NS-50 %RS1, (c) 100 %RS1, (d) 50 %NS-50 %RS2 and (e) 100 %RS2.

analysed by TD NMR as:

$$water_{hydrates} = m_{NMR} \bullet (1 - WA\%) \bullet 0.11$$

With this approach, the water coming from sample curing was assumed to contribute to larger pores, higher than 7 nm, thus detected by MIP. The calculation of the volume of water occupied by pores larger than 7 nm in TD NMR sample, V_{MIP}, was conducted by estimating the geometric volume of TD NMR samples:

$$V_{bulk-NMR} = \frac{m_{NMR} \bullet (1 - WA\%)}{\rho_{bulk}}$$

Then, this volume multiplied by the open porosity detected by MIP, $OP_{MIP}\%$, provides the volume of water in pores detected by TD NMR and also detected by MIP:

$$V_{MIP} = V_{bulk-NMR} \bullet OP_{MIP}\%$$

Assuming water density $\rho_{water} = 1g/cm^3$ this can be converted in mass:

$$water_{MIP-pores} = V_{MIP} \bullet \rho_{water}$$

Assuming that the total amount of water detected by TD NMR is the sum of water in hydrates and the water in pores larges than 7 nm, detected by MIP, the following equation provide a percentage of the water contained in pores detected by MIP:

$$water_{MIP-pores} \quad \% = \frac{water_{MIP-pores}}{water_{hydrates} + water_{MIP-pores}} \bullet 100$$

All the explicated calculations are reported in Table 7 for mortars prepared with NS.

The water percentage contained in pores detected by MIP is between 30 % and 36 % of the water detected by TD NMR. A specific software developed at University of Bologna was used to calculate the percentage of the T_2 distribution corresponding to the $water_{MIP-pores}\%$ in order identify the corresponding relaxation time. These values correspond to the relaxation time distinguishing between the population of pores detected by MIP and the C-S-H pores detected by TD NMR. The obtained

Table 7
– Calculation of the comparison between MIP and NMR detected porosity for mortar prepared with NS.

Measured/calculated quantities	CEM I	CEM II	LC3-50 2:1	LC3-50 1:1	LC3-70 2:1
ρ_{bulk} (g/cm^3)	2.167	2.048	2.155	2.113	2.07
OP_{MIP}% (%)	12.19	14.41	14.06	14.03	11.61
WA% (%)	6.9	7.9	7.3	7.9	7.3
m_{NMR} (g)	19.35	25.49	18.54	20.03	17.57
$water_{hydrates}$ (g)	2.00	2.61	1.91	2.05	1.81
$V_{bulk-NMR}$ (cm^3)	7.70	9.99	7.48	7.83	6.92
V_{MIP} (cm^3)	0.94	1.44	1.05	1.10	0.80
$water_{MIP-pores}$ (g)	0.94	1.44	1.05	1.10	0.80
$water_{MIP-pores}$ % (%)	31.9	35.6	35.5	34.9	30.7

values are slightly varying from one binder to the other and they are in a range between 0.21 and 0.29 ms. This relaxation time well correspond to the C-S-H interlayer water highly visible at 28 days of hydration.

Concluding, the presented approach allowed the comparison of the mortar porosity assessment performed by MIP and TD NMR. It was calculated that, in the analysed specimens, MIP identifies around 30–36 % of the porosity detected by TD NMR. This is coherent with the limit of detection of both instruments and the previous literature in the field.

The economic feasibility and environmental benefits of using LC^3 and recycled sand in mortar for concrete are significant [95]. Environmentally, LC^3 has a lower carbon footprint compared to traditional Portland cement, as its production emits up to 40 % less CO_2 due to the reduced clinker content and the energy-efficient process of calcining clay. Incorporating recycled sand further enhances the sustainability profile by recycling waste from landfills and reducing the need for natural sand extraction, which is associated with habitat destruction and energy consumption [96]. Therefore, mortar containing LC^3 and recycled sand presents a promising alternative in the construction industry, balancing cost-effectiveness with ecological responsibility and performances.

4. Conclusions

This study reports the performances of mortars prepared with a combination of LC^3 with recycled sands. The results obtained for mortars manufactured with various binders in combination with 50 % and 100 % RS1 and RS2 were compared to those obtained for mortar prepared with NS. Two commercial cements, CEM I and CEM II, were used as reference binders. The results obtained in the experimental testing can be summarised as follows:

1) The workability of the mortars remained basically unaffected by the incorporation of recycled sand because the sand replacement was carried out by volume rather than by mass.
2) The substitution rate of recycled sand gradually decreased the mechanical properties. However, mortars with LC^3-70–2:1 binder showed superior 28 days compressive strength in comparison to those with CEM I for NS and RS1, and superior 28 days compressive strength in comparison to those with CEM II for all levels of RS1 and RS2 replacement, thus compensating the loss of performances due to the employment of recycled sand.
3) The combination of calcined clay and limestone in binder can significantly reduce water capillary absorption coefficient, with NS but also with RS. In fact, LC^3 fully compensated the negative effect provided by recycled sand in terms of capillary water absorption rate.
4) The MIP analysis revealed that mortars with LC3–70 2:1-NS, LC3–70 2:1–50RS1, and LC3–70 2:1–100RS1 have reduced total porosity and a more refined pore network. As a result, these mortars demonstrate superior mechanical and durability properties compared to CEM I-NS, CEM I-50RS1, CEM I-100RS1, and CEM II-NS, CEM II-50RS1, and CEM II-100RS1.
5) The TD NMR provides complementary information about the mortars' pores relative to MIP, detecting the presence of finer gel pores in LC3–70 2:1 compared to CEM II. This explains the higher mechanical strength observed in LC3–70 2:1.
6) The comparison between MIP and TD NMR technique allowed to estimate that the porosity percentage detected by classical method (MIP) can reach only 30–36 % of the total water-filled voids detectable by TD NMR.
7) LC^3 binders can be used instead of commercially available cements, where the rate of water absorption is a critical factor, and this becomes even more significant if recycled aggregates are used for mortar preparation.

These findings collectively contribute to a deeper understanding of the complex interplay between materials and water absorption, especially highlighting the great advantage of combining LC^3 with recycled sands. Indeed, not only LC^3 reaches satisfying performances in comparison to commercial cements, at fresh and hardened state, but also, in mixes containing recycled sand, it compensates the negative effect of RS on mechanical strength and water absorption. This research sheds light on potential improvements in sustainability of cement and mortar formulations, paving the way for greener construction practices and promoting the development of more sustainable materials for infrastructures.

CRediT authorship contribution statement

Ahmad Jan: Writing – original draft, Methodology, Formal analysis, Data curation. **Lucia Ferrari:** Writing – review & editing, Writing – original draft, Supervision, Investigation, Funding acquisition, Formal analysis, Data curation, Conceptualization. **Villiam Bortolotti:** Writing – review & editing, Supervision, Investigation, Formal analysis. **Nikola Mikanovic:** Writing – review & editing, Supervision, Methodology. **Mohsen Ben-Haha:** Writing – review & editing, Supervision, Project administration, Funding acquisition, Conceptualization. **Elisa Franzoni:** Writing – review & editing, Supervision, Project administration, Methodology, Funding acquisition, Data curation, Conceptualization.

Declaration of Competing Interest

The authors declare the following financial interests/personal relationships which may be considered as potential competing interests: Lucia Ferrari reports financial support was provided by Heidelberg Materials AG. If there are other authors, they declare that they have no known competing financial interests or personal relationships that could have appeared to influence the work reported in this paper.

Data Availability

Data will be made available on request.

Acknowledgments

The authors would like to acknowledge Heidelberg Materials AG for financial support. Andrea Sgaravatto from University of Bologna is warmly thanked for his support during laboratory tests. Giovanni Ridolfi from CentroCeramico is thanked for providing the analysis of particle size distribution of calcined clay and limestone.

Annex A

Table A-Mechanical Strength Properties of mortars with NS, RS1, RS2

Series	Samples	Flexural Strength (MPa)		Compressive strength (MPa)	
		2 Days	28 Days	2 Days	28 Days
NS	CEM I	7.8 (±0.2)	12.2 (±0.6)	50.5 (±0.5)	68.9 (±0.4)
	CEM II	7.3 (±0.1)	11.3 (±0.4)	38.0 (±0.2)	56.5 (±0.1)
	LC3–50 2:1	7.0 (±0.7)	11.6 (±0.6)	33.4 (±0.1)	63.8 (±0.4)
	LC3–50 1:1	7.5 (±0.1)	12.2 (±0.5)	28.6 (±0.5)	61.9 (±0.5)
	LC3–70 2:1	8.8 (±0.4)	12.1 (±0.1)	41.7 (±0.5)	76.5 (±0.6)
50 % RS1	CEM I	7.6 (±0.4)	10.2 (±0.1)	43.6 (±0.2)	63.1 (±0.2)
	CEM II	7.9 (±0.3)	9.4 (±0.5)	29.8 (±0.1)	50.4 (±0.2)
	LC3–50 2:1	5.2 (±0.1)	9.6 (±0.3)	19.4 (±0.1)	55.1 (±0.1)
	LC3–50 1:1	5.4 (±0.2)	10.1 (±0.1)	19.2 (±0.1)	52.8 (±0.3)
	LC3–70 2:1	7.9 (±0.2)	9.2 (±0.4)	32.2 (±0.3)	63.4 (±0.1)
100 % RS1	CEM I	6.1 (±0.8)	7.3 (±0.1)	35.6 (±0.5)	43.7 (±0.5)
	CEM II	5.8 (±0.7)	8.1 (±0.3)	26.3 (±0.3)	40.0 (±0.3)
	LC3–50 2:1	5.0 (±0.3)	8.1 (±0.2)	19.6 (±0.1)	49.5 (±0.2)
	LC3–50 1:1	4.1 (±1.1)	7.8 (±0.2)	17.6 (±0.1)	45.2 (±0.3)
	LC3–70 2:1	6.5 (±0.2)	8.7 (±0.9)	30.4 (±0.1)	55.0 (±0.5)
50 % RS2	CEM I	7.0 (±0.4)	8.9 (±0.3)	39.2 (±0.1)	60.8 (±0.2)
	CEM II	6.6 (±0.4)	9.2 (±0.4)	28.8 (±0.1)	50.4 (±0.2)
	LC3–50 2:1	4.2 (±0.0)	8.2 (±0.1)	19.9 (±0.1)	46.1 (±0.2)
	LC3–50 1:1	3.8 (±0.1)	8.2 (±0.4)	18.3 (±0.1)	41.6 (±0.1)
	LC3–70 2:1	5.5 (±0.5)	8.5 (±0.2)	27.5 (±0.2)	53.5 (±0.3)
100 % RS2	CEM I	5.7 (±0.5)	8.1 (±0.3)	27.6 (±0.2)	44.3 (±0.3)
	CEM II	5.5 (±0.2)	8.1 (±0.4)	22.2 (±0.1)	40.9 (±0.1)
	LC3–50 2:1	2.9 (±0.1)	5.9 (±0.1)	14.8 (±0.1)	34.7 (±0.1)
	LC3–50 1:1	2.9 (±0.2)	7.5 (±0.3)	13.2 (±0.1)	34.4 (±0.1)
	LC3–70 2:1	4.6 (±0.1)	7.5 (±0.2)	20.9 (±0.1)	41.2 (±0.2)

References

[1] Environment, U., K.L. Scrivener, V.M. John, E.M.J.C. Gartner, and c Research, Eco-efficient cements: Potential economically viable solutions for a low-CO2 cement-based materials industry. 2018. 114: p. 2-26.

[2] Jan, A., Z. Pu, K.A. Khan, I. Ahmad, A.J. Shaukat, Z. Hao, and I.J.S. Khan, A review on the effect of silica to alumina ratio, alkaline solution to binder ratio, calcium oxide+ ferric oxide, molar concentration of sodium hydroxide and sodium silicate to sodium hydroxide ratio on the compressive strength of geopolymer concrete. 2022. 14(7): p. 3147-3162.

[3] U.S. Geological Survey (2014). Mineral commodity summaries 2014. Mineral Commodity Summaries. https://doi.org/⟨10.3133/70100414⟩.

[4] International Energy Agency, Technology Roadmap: Low-Carbon Transition in the Cement Industry, 2018.

[5] B. Lothenbach, K. Scrivener, R.D. Hooton, Supplementary cementitious materials, Cem. Concr. Res. 41 (12) (2011) 1244–1256, https://doi.org/10.1016/j.cemconres.2010.12.001.

[6] G. Chand, Microstructural study of sustainable cements produced from industrial by-products, natural minerals and agricultural wastes: a critical review on engineering properties, Clean. Eng. Technol. 4 (2021) 100224.

[7] Scrivener, K., F. Martirena, S. Bishnoi, S.J.C. Maity, and C. research, Calcined clay limestone cements (LC3). 2018. 114: p. 49-56.

[8] M. Sharma, S. Bishnoi, F. Martirena, K. Scrivener, Limestone calcined clay cement and concrete: a state-of-the-art review, Cem. Concr. Res. 149 (2021) 106564.

[9] M.H. Guo, G.Q. Gong, Y.C. Yue, F. Xing, Y.W. Zhou, B. Hu, Performance evaluation of recycled aggregate concrete incorporating limestone calcined clay cement (LC), J. Clean. Prod. 366 (2022) 132820.

[10] R. Fernandez, F. Martirena, K.L. Scrivener, The origin of the pozzolanic activity of calcined clay minerals: a comparison between kaolinite, illite and montmorillonite, Cem. Concr. Res. 41 (1) (2011) 113–122, https://doi.org/10.1016/j.cemconres.2010.09.013.

[11] Ptáček, P., F. Frajkorová, F. Šoukal, and T.J.P.T. Opravil, Kinetics and mechanism of three stages of thermal transformation of kaolinite to metakaolinite. 2014. 264: p. 439-445.

[12] A. Tironi, M.A. Trezza, A.N. Scian, E.F. Irassar, Assessment of pozzolanic activity of different calcined clays, Cem. Concr. Compos. 37 (2013) 319–327, https://doi.org/10.1016/j.cemconcomp.2013.01.002.

[13] Silva, A.S., A. Gameiro, J. Grilo, R. Veiga, and A.J.A.C.S. Velosa, Long-term behavior of lime–metakaolin pastes at ambient temperature and humid curing condition. 2014. 88: p. 49-55.

[14] B. Lothenbach, G. Le Saout, E. Gallucci, K. Scrivener, Influence of limestone on the hydration of portland cements, Cem. Concr. Res. 38 (6) (2008) 848–860, https://doi.org/10.1016/j.cemconres.2008.01.002.

[15] F. Avet, K. Scrivener, Investigation of the calcined kaolinite content on the hydration of Limestone Calcined Clay Cement (LC), Cem. Concr. Res. 107 (2018) 124–135, https://doi.org/10.1016/j.cemconres.2018.02.016.

[16] M. Antoni, J. Rossen, F. Martirena, K. Scrivener, Cement substitution by a combination of metakaolin and limestone, Cem. Concr. Res. 42 (12) (2012) 1579–1589, https://doi.org/10.1016/j.cemconres.2012.09.006.

[17] 197–5, E., Cement - Part 5: Portland-composite cement CEM II/CM and Composite cement CEM VI. 2021.

[18] Y. Dhandapani, S. Joseph, D.A. Geddes, Z. Zhao, P. Boustingorry, S. Bishnoi, M. Vieira, F. Martirena, A. Castel, F. Kanavaris, K.A. Riding, Fresh properties of concrete containing calcined clays: a review by RILEM TC-282 CCL, Mater. Struct. 55 (6) (2022) 151.

[19] C. Aramburo, C. Pedrajas, V. Rahhal, M. González, R. Talero, Calcined clays for low carbon cement: Rheological behaviour in fresh Portland cement pastes, Mater. Lett. 239 (2019) 24–28, https://doi.org/10.1016/j.matlet.2018.12.050.

[20] B. Lorentz, N. Shanahan, A. Zayed, Rheological behavior & modeling of calcined kaolin-Portland cements, in: Construction and Building Materials, 307, 2021 124761.

[21] N. Nair, K.M. Haneefa, M. Santhanam, R. Gettu, A study on fresh properties of limestone calcined clay blended cementitious systems, in: Construction and Building Materials, 254, 2020 119326.

[22] T.R. Muzenda, P.K. Hou, S. Kawashima, T.B. Sui, X. Cheng, The role of limestone and calcined clay on the rheological properties of LC3, Cem. Concr. Compos. 107 (2020) 103516.

[23] P.K. Hou, T.R. Muzenda, Q.F. Li, H. Chen, S. Kawashima, T.B. Sui, H.Y. Yong, N. Xie, X. Cheng, Mechanisms dominating thixotropy in limestone calcined clay cement (LC3), in: Cement and Concrete Research, 140, 2021 106316.

[24] Ferrari, L., V. Bortolotti, N. Mikanovic, M. Ben-Haha, and E. Franzoni, Influence of low carbon cement and recycled aggregates on mortar fresh state and early hydration.

[25] C. Schiefer, J. Plank, On the CO footprint of polycarboxylate superplasticizers (PCEs) and its impact on the eco balance of concrete, in: Construction and Building Materials, 409, 2023 133944.

[26] M. Schmid, J. Plank, Interaction of individual meta clays with polycarboxylate (PCE) superplasticizers in cement investigated via dispersion, zeta potential and sorption measurements, Appl. Clay Sci. 207 (2021) 106092.

[27] M. Schmid, J. Plank, Dispersing performance of different kinds of polycarboxylate (PCE) superplasticizers in cement blended with a calcined clay, in: Construction and Building Materials, 258, 2020 119576.

[28] R. Li, L. Lei, J. Plank, Influence of PCE superplasticizers on the fresh properties of low carbon cements containing calcined clays: A comparative study of calcined clays from three different sources, Cem. Concr. Compos. 139 (2023) 105072.

[29] R. Li, L. Lei, T.B. Sui, J. Plank, Approaches to achieve fluidity retention in low-carbon calcined clay blended cements, J. Clean. Prod. 311 (2021) 127770.

[30] R. Li, L. Lei, T.B. Sui, J. Plank, Effectiveness of PCE superplasticizers in calcined clay blended cements, Cem. Concr. Res. 141 (2021) 106334.

[31] R. Sposito, M. Maier, N. Beuntner, K.C. Thienel, Evaluation of zeta potential of calcined clays and time-dependent flowability of blended cements with customized polycarboxylate-based superplasticizers, Constr. Build. Mater. 308 (2021) 125061.

[32] O. Akhlaghi, T. Aytas, B. Tatli, D. Sezer, A. Hodaei, A. Favier, K. Scrivener, Y. Z. Menceloglu, O. Akbulut, Modified poly(carboxylate ether)-based superplasticizer for enhanced flowability of calcined clay-limestone-gypsum blended Portland cement, Cem. Concr. Res. 101 (2017) 114–122, https://doi.org/10.1016/j.cemconres.2017.08.028.

[33] S. Krishnan, Hydration and Microstructure Development in Limestone Calcined Clay Cement, IIT Delhi, 2019.

[34] Y. Dhandapani, T. Sakthivel, M. Santhanam, R. Gettu, R.G. Pillai, Mechanical properties and durability performance of concretes with Limestone Calcined Clay Cement (LC), Cem. Concr. Res. 107 (2018) 136–151, https://doi.org/10.1016/j.cemconres.2018.02.005.

[35] S. Krishnan, S. Bishnoi, A numerical approach for designing composite cements with calcined clay and limestone, Cem. Concr. Res. 138 (2020) 106232.

[36] G. Mishra, A.C. Emmanuel, S. Bishnoi, Influence of temperature on hydration and microstructure properties of limestone-calcined clay blended cement, Mater. Struct. 52 (5) (2019) 1–13.

[37] Maraghechi, H., F. Avet, H. Wong, H. Kamyab, K.J.M. Scrivener, and structures, Performance of Limestone Calcined Clay Cement (LC 3) with various kaolinite contents with respect to chloride transport. 2018. 51: p. 1-17.

[38] Shi, Z., S. Ferreiro, B. Lothenbach, M.R. Geiker, W. Kunther, J. Kaufmann, D. Herfort, J.J.C. Skibsted, and C. Research, Sulfate resistance of calcined clay–Limestone–Portland cements. 2019. 116: p. 238-251.

[39] Y. Dhandapani, S. Joseph, S. Bishnoi, W. Kunther, F. Kanavaris, T. Kim, E. Irassar, A. Castel, F. Zunino, A. Machner, V. Talakokula, K.C. Thienel, W. Wilson, J. Elsen, F. Martirena, M. Santhanam, Durability performance of binary and ternary blended cementitious systems with calcined clay: a RILEM TC 282 CCL review, Mater. Struct. 55 (5) (2022) 145.

[40] Harshvardhan, A.C. Emmanuel, S. Bishnoi, Assessment of sorptivity and porosity characteristics of self-compacting concrete from blended cements using calcined clay and Fly Ash at various replacement levels. Calcined Clays for Sustainable Concrete: Proceedings of the 3rd International Conference on Calcined Clays for Sustainable Concrete, Springer, 2020.

[41] F. Bahman-Zadeh, A.A. Ramezanianpour, A. Zolfagharnasab, Effect of carbonation on chloride binding capacity of limestone calcined clay cement (LC3) and binary pastes, J. Build. Eng. 52 (2022) 104447.

[42] F. Zunino, K. Scrivener, The reaction between metakaolin and limestone and its effect in porosity refinement and mechanical properties, Cem. Concr. Res. 140 (2021) 106307.

[43] Z. Shi, M.R. Geiker, K. De Weerdt, B. Lothenbach, J. Kaufmann, W. Kunther, S. Ferreiro, D. Herfort, J. Skibsted, Durability of Portland cement blends including calcined clay and limestone: interactions with sulfate, chloride and carbonate ions. Calcined Clays for Sustainable Concrete: Proceedings of the 1st International Conference on Calcined Clays for Sustainable Concrete, Springer, 2015.

[44] F. Almeida, J.R. Carneiro, M.D. Lopes, Use of incinerator bottom ash as a recycled aggregate in contact with nonwoven geotextiles: evaluation of mechanical damage upon installation, Sustainability 12 (21) (2020) 9156.

[45] Eurostat. Waste Statistics. Available online: ⟨https://ec.europa.eu/eurostat/statistics-explained/index.php?title=Waste_statistics⟩.

[46] M. Bendixen, J. Best, C. Hackney, L.L. Iversen, Time is running out for sand, Nature 571 (7763) (2019) 29–31, https://doi.org/10.1038/d41586-019-02042-4.

[47] P. Peduzzi, Sand, rarer than one thinks, Environ. Dev. 11 (208-218) (2014) 682.

[48] G.H. Allen, T.M. Pavelsky, Global extent of rivers and streams, Science 361 (6402) (2018) 585–588, https://doi.org/10.1126/science.aat0636.

[49] Ghorbel, E., G. Wardeh, H. Gomart, and P.J.Jo.B.P. Matar, Formulation parameters effects on the performances of concrete equivalent mortars incorporating different ratios of recycled sand. 2020. 43(6): p. 545-572 DOI: ⟨10.1177/1744259119896093⟩.

[50] C.Q. Wang, J.Z. Xiao, W.G. Liu, Z.M. Ma, Unloading and reloading stress-strain relationship of recycled aggregate concrete reinforced with steel/polypropylene fibers under uniaxial low-cycle loadings, Cem. Concr. Compos. 131 (2022) 104597.

[51] Santos, M.B., J. De Brito, A.S. Silva, A.J.C. Hawreen, and C. Composites, Effect of the source concrete with ASR degradation on the mechanical and physical properties of coarse recycled aggregate. 2020. 111: p. 103621.

[52] Guo, H., C. Shi, X. Guan, J. Zhu, Y. Ding, T.-C. Ling, H. Zhang, Y.J.C. Wang, and c. composites, Durability of recycled aggregate concrete–A review. 2018. 89: p. 251-259.

[53] P.H. Zhu, Y.L. Hao, H. Liu, X.J. Wang, L. Gu, Durability evaluation of recycled aggregate concrete in a complex environment, J. Clean. Prod. 273 (2020) 122569.

[54] J. Lavado, J. Bogas, J. de Brito, A. Hawreen, Fresh properties of recycled aggregate concrete, Constr. Build. Mater. 233 (2020) 117322.

[55] A. Karimipour, M. Edalati, RETRACTED: influence of untreated coal and recycled aggregates on the mechanical properties of green concrete, Elsevier, 2020.

[56] C.F. Lu, Q.S. Zhou, W. Wang, S.H. Wei, C. Wang, Freeze-thaw resistance of recycled aggregate concrete damaged by simulated acid rain, J. Clean. Prod. 280 (2021) 124396.

[57] Santha Kumar, G., P. Saini, S. Karade, A.J.Jo.M.C. Minocha, and W. Management, Chemico-thermal treatment for quality enhancement of recycled concrete fine aggregates. 2019. 21: p. 1197-1210.

[58] L. Li, D.X. Xuan, S.H. Chu, J.X. Lu, C.S. Poon, Efficiency and mechanism of nano-silica pre-spraying treatment in performance enhancement of recycled aggregate concrete, Constr. Build. Mater. 301 (2021) 124093. DOI: ARTN 12409310.1016/j.conbuildmat.2021.124093.

[59] Shaban, W.M., J. Yang, H. Su, K.H. Mo, L. Li, and J.J.Jo.A.C.T. Xie, Quality improvement techniques for recycled concrete aggregate: A review. 2019. 17(4): p. 151-167.

[60] G. Chinzorigt, M.K. Lim, M. Yu, H. Lee, O. Enkbold, D. Choi, Strength, shrinkage and creep and durability aspects of concrete including CO treated recycled fine aggregate, Cem. Concr. Res. 136 (2020) 106062.

[61] Y.C. Tang, C. Zheng, W.H. Feng, Y.M. Nong, L. Cong, J.M. Chen, Combined effects of nano-silica and silica fume on the mechanical behavior of recycled aggregate concrete, Nanotechnol. Rev. 10 (1) (2021) 819–838.

[62] X.B. Song, C.Z. Li, D.D. Chen, X.L. Gu, Interfacial mechanical properties of recycled aggregate concrete reinforced by nano-materials, Constr. Build. Mater. 270 (2021) 121446.

[63] Z.M. Ma, J.X. Shen, C.Q. Wang, H.X. Wu, Characterization of sustainable mortar containing high-quality recycled manufactured sand crushed from recycled coarse aggregate, Cem. Concr. Compos. 132 (2022) 104629, https://doi.org/10.1016/j.cemconcomp.2022.104629.

[64] Z. Zhao, S. Remond, D. Damidot, L. Courard, Une nouvelle méthode de caractérisation des granulats recyclés industriels: application aux mortiers et bétons, 2015. in NoMaD, IMT Mines douai, 2015.

[65] T. Le, S. Rémond, G. Le Saout, E. Garcia-Diaz, Fresh behavior of mortar based on recycled sand – Influence of moisture condition, Constr. Build. Mater. 106 (2016) 35–42, https://doi.org/10.1016/j.conbuildmat.2015.12.071.

[66] Z. Zhao, S. Remond, D. Damidot, W. Xu, Influence of fine recycled concrete aggregates on the properties of mortars, Constr. Build. Mater. 81 (2015) 179–186, https://doi.org/10.1016/j.conbuildmat.2015.02.037.

[67] S.K. Kirthika, S.K. Singh, Durability studies on recycled fine aggregate concrete, Constr. Build. Mater. 250 (2020) 118850, https://doi.org/10.1016/j.conbuildmat.2020.118850.

[68] Raut, S., S. Olcun, and L.J.J.M.T.P. Butler, Evaluating the use of limestone calcined clay cement and recycled concrete aggregates for reducing the carbon footprint of concrete structures. 2023.

[69] H. Alghamdi, H. Shoukry, A.A. Abadel, M. Khawaji, Performance assessment of limestone calcined clay cement (LC3)-based lightweight green mortars incorporating recycled waste aggregate, J. Mater. Res. Technol. -JmrT 23 (2023) 2065–2074, https://doi.org/10.1016/j.jmrt.2023.01.133.

[70] D.C. Guo, M.H. Guo, F. Xing, Y.W. Zhou, Z.Y. Huang, W.L. Cao, Using limestone calcined clay cement and recycled fine aggregate to make ultra-high-performance concrete: properties and environmental impact, Constr. Build. Mater. 394 (2023) 132026.

[71] Muller, A.C., K.L. Scrivener, A.M. Gajewicz, and P.J.J.T.Jo.P.C.C. McDonald, Densification of C–S–H measured by 1H NMR relaxometry. 2013. 117(1): p. 403-412.

[72] Nagmutdinova, A., L. Brizi, P. Fantazzini, and V.J.A.M.R. Bortolotti, Investigation of the first sorption cycle of white portland cement by 1h NMR. 2021. 52: p. 1767-1785.

[73] Y. Briki, F. Avet, M. Zajac, P. Bowen, M. Ben Haha, K. Scrivener, Understanding of the factors slowing down metakaolin reaction in limestone calcined clay cement (LC) at late ages, in: Cement and Concrete Research, 146, 2021 106477.

[74] Skocek, J., A. Ouzia, E. Vargas, and N. Pato, Recycled sand and aggregates for structural concrete. Available at SSRN 4549471, 2023.

[75] EN, 933–1: Tests for geometrical properties of aggregates - Part 1: Determination of particle size distribution - Sieving method. 2012.

[76] EN, 1097–6: Tests for mechanical and physical properties of aggregates - Part 6: Determination of particle density and water absorption. 2022.

[77] EN, B., 933–9:, Tests for geometrical properties of aggregates - Assessment of fines. Methylene blue test. 2022.

[78] EN, 1015–11 Methods of test for masonry - Part 11: Determination of flexural and compressive strength of hardened mortar, in EUROPEAN COMMITTEE FOR STANDARDIZATION (CEN). 1999.

[79] UNI, EN 196–1:2016 Test methods for cements - Part 1: Determination of mechanical resistance.

[80] EN, 197–1 Cement - Part 1: Composition, specifications and conformity criteria for common cements. 2011.

[81] EN, 1015–18 Methods of test for mortar for masonry - Part 18: Determination of water absorption coefficient due to capillary action of hardened mortar, in EUROPEAN COMMITTEE FOR STANDARDIZATION (CEN). 2002.

[82] ASTM, C 642–13, Standard test method for density, absorption, and voids in hardened concrete.

[83] V. Bortolotti, R.J.S. Brown, and P. Fantazzini, "UpenWin A software for inversion of multiexponential decay datafor Windows system," Alma Mater Studiorum – Università di Bologna.

[84] Ferrari, L., V. Bortolotti, N. Mikanovic, M. Ben-Haha, and E.J.N.J. Franzoni, Influence of Calcined Clay on Workability of Mortars with Low-carbon Cement. 2023. 9(S2): p. S30-S34.

[85] Dhers, S., A. Müller, R. Guggenberger, D. Freimut, K. Weldert, B. Sachsenhauser, V. Yermakou, N. Mikanovic, P.J.C. Schwesig, and B. Materials, On the relationship between superplasticizer demand and specific surface area of calcined clays in LC3 systems. 2024. 411: p. 134467.

[86] R.-S. Lin, H.-S. Lee, Y. Han, X.-Y. Wang, Experimental studies on hydration–strength–durability of limestone-cement-calcined Hwangtoh clay ternary composite, Constr. Build. Mater. 269 (2021) 121290.

[87] R.-S. Lin, S. Oh, W. Du, X.-Y. Wang, Strengthening the performance of limestone-calcined clay cement (LC3) using nano silica, Constr. Build. Mater. 340 (2022) 127723, https://doi.org/10.1016/j.conbuildmat.2022.127723.

[88] K. Scrivener, F. Martirena, S. Bishnoi, S. Maity, Calcined clay limestone cements (LC3), Cem. Concr. Res. 114 (2018) 49–56.

[89] F. Avet, K. Scrivener, Investigation of the calcined kaolinite content on the hydration of Limestone Calcined Clay Cement (LC3), Cem. Concr. Res. 107 (2018) 124–135, https://doi.org/10.1016/j.cemconres.2018.02.016.
[90] Y. Dhandapani, T. Sakthivel, M. Santhanam, R. Gettu, R.G. Pillai, Mechanical properties and durability performance of concretes with limestone calcined clay cement (LC3), Cem. Concr. Res. 107 (2018) 136–151, https://doi.org/10.1016/j.cemconres.2018.02.005.
[91] A. Zolfagharnasab, A.A. Ramezanianpour, F. Bahman-Zadeh, Investigating the potential of low-grade calcined clays to produce durable LC3 binders against chloride ions attack, Constr. Build. Mater. 303 (2021) 124541, https://doi.org/10.1016/j.conbuildmat.2021.124541.
[92] Z. Li, J.P. Liu, J.Z. Xiao, P.H. Zhong, A method to determine water absorption of recycled fine aggregate in paste for design and quality control of fresh mortar, Constr. Build. Mater. 197 (2019) 30–41, https://doi.org/10.1016/j.conbuildmat.2018.11.115.
[93] A.M. Gajewicz, E. Gartner, K. Kang, P.J. McDonald, V. Yermakou, A ^{1}H NMR relaxometry investigation of gel-pore drying shrinkage in cement pastes, Cem. Concr. Res. 86 (2016) 12–19, https://doi.org/10.1016/j.cemconres.2016.04.013.
[94] A.M. Gajewicz, E. Gartner, K. Kang, P.J. McDonald, V. Yermakou, A H NMR relaxometry investigation of gel-pore drying shrinkage in cement pastes, Cem. Concr. Res. 86 (2016) 12–19, https://doi.org/10.1016/j.cemconres.2016.04.013.
[95] B. Kanagaraj, N. Anand, U. Johnson Alengaram, R. Samuvel Raj, S. Karthick, Limestone calcined clay cement (LC3): A sustainable solution for mitigating environmental impact in the construction sector, Resour., Conserv. Recycl. Adv. 21 (2024) 200197, https://doi.org/10.1016/j.rcradv.2023.200197.
[96] J. Nilimaa, Smart materials and technologies for sustainable concrete construction, Dev. Built Environ. 15 (2023) 100177, https://doi.org/10.1016/j.dibe.2023.100177.